



HHS Public Access

Author manuscript

Pain. Author manuscript; available in PMC 2017 October 25.

Published in final edited form as:

Pain. 2017 April ; 158(4): 747–759. doi:10.1097/j.pain.0000000000000830.

Divergent functions of the left and right central amygdala in visceral nociception

Katelyn E. Sadler, Neal A. McQuaid, Abigail C. Cox, Marissa N. Behun, Allison M. Trouten, and Benedict J. Kolber*

Department of Biological Sciences and Chronic Pain Research Consortium, Duquesne University, Pittsburgh, PA, USA

Abstract

The left and right central amygdalae (CeA) are limbic regions involved in somatic and visceral pain processing. These 2 nuclei are asymmetrically involved in somatic pain modulation; pain-like responses on both sides of the body are preferentially driven by the right CeA, and in a reciprocal fashion, nociceptive somatic stimuli on both sides of the body predominantly alter molecular and physiological activities in the right CeA. Unknown, however, is whether this lateralization also exists in visceral pain processing and furthermore what function the left CeA has in modulating nociceptive information. Using urinary bladder distension (UBD) and excitatory optogenetics, a pronociceptive function of the right CeA was demonstrated in mice. Channelrhodopsin-2-mediated activation of the right CeA increased visceromotor responses (VMRs), while activation of the left CeA had no effect. Similarly, UBD-evoked VMRs increased after unilateral infusion of pituitary adenylate cyclase-activating polypeptide in the right CeA. To determine intrinsic left CeA involvement in bladder pain modulation, this region was optogenetically silenced during noxious UBD. Halorhodopsin (NpHR)-mediated inhibition of the left CeA increased VMRs, suggesting an ongoing antinociceptive function for this region. Finally, divergent left and right CeA functions were evaluated during abdominal mechanosensory testing. In naive animals, channelrhodopsin-2-mediated activation of the right CeA induced mechanical allodynia, and after cyclophosphamide-induced bladder sensitization, activation of the left CeA reversed referred bladder pain-like behaviors. Overall, these data provide evidence for functional brain lateralization in the absence of peripheral anatomical asymmetries.

Keywords

Neuroscience; Mouse; Amygdala; Bladder; PACAP; Lateralization

*Corresponding author. Address: Department of Biological Sciences, 600 Forbes Ave, Mellon Hall 260, Pittsburgh, PA 15282, USA. Tel.: 412-396-5615. E-mail address: kolberb@duq.edu (B. J. Kolber).

Conflict of interest statement

The authors have no conflicts of interest to declare.

The authors declare no competing financial interests.

1. Introduction

Chronic bladder pain, often diagnosed as interstitial cystitis/bladder pain syndrome or chronic prostatitis/chronic pelvic pain syndrome, is characterized by sensory and emotional dysfunction.^{25,34} These discrete symptoms are simultaneously processed by limbic brain circuits that include the central amygdala (CeA), an area that integrates convergent projections from cortical, sub-cortical, and brainstem regions.³³ Recent brain imaging studies in patients with chronic bladder pain have reported hemispheric asymmetries in amygdala structural integrity, anatomical connectivity, and functional activity.^{1,3,16,27} These data are noteworthy because noxious bladder signals are presumed to equally engage both sides of the brain through bilateral peripheral and spinal afferents.^{10,36}

To date, few preclinical rodent studies have adequately addressed the hemispheric discrepancies observed in clinical bladder pain populations. Most studies have bilaterally manipulated or observed CeA activities during bladder nociception.^{5,14,35} For instance, bilateral CeA lesions prevent the generation of stress-induced bladder hyperalgesia in rats, but it is unknown if this mechanism is specific to the left or right CeA or requires bilateral input.¹⁴ In one exception, global optogenetic activation of the right CeA and pharmacological activation of metabotropic glutamate receptors 1/5 (mGluR1/5) within this nucleus increased pain-like responses to urinary bladder distension (UBD), suggesting a pronociceptive function of the CeA.¹³ However, these manipulations were only performed in the right hemisphere, leaving the functional implications of similar left CeA activities unknown.

Central amygdala lateralization has previously been reported in somatic pain. In contrast to bladder nociception, noxious somatic information is transmitted through unilateral projection systems, engaging only one side of the brain.⁵⁰ It was thus surprising when preferential activation of the right CeA was noted in several rodent somatic pain models; both experimental arthritis and peripheral inflammation increased nociceptive activities in the right CeA, regardless of the side of injury.^{9,23} Following this trend, activation of mGluR5 in the right CeA induced both contralateral and ipsilateral peripheral hypersensitivity in the absence of injury, while left CeA activation only induced contralateral hypersensitivity.³⁷ It is unknown if this same functional lateralization exists in visceral nociceptive processing since no study has examined the effects of equal unilateral CeA manipulations on visceral pain.

Here, we specifically addressed the contributions of the left and right CeA to bladder pain modulation. Using excitatory optogenetics, we unilaterally activated the left and right CeA to learn how each nucleus modulated bladder nociception. We also examined the specific functions of pituitary adenylate cyclase-activating polypeptide (PACAP), a peptide released by para-brachial nucleus (PBn) terminals in the CeA, within each nucleus during graded bladder distension. The endogenous nociceptive functions of the left and right CeA were investigated during noxious bladder stimulation using inhibitory optogenetics. Finally, inflammation-induced changes in the left and right CeA functions were explored in 2 rodent bladder pain assessments. Overall, these studies demonstrate lateralized activities for the left

and right CeA in the context of visceral bladder pain that are unique from those observed in somatic pain.

2. Methods

2.1. Animals

Female mice aged 7 to 12 weeks were used for all the experiments. All animals were on a C57Bl/6J background. All animals were bred in house; mating pairs were acquired from Jackson Laboratory (Bar Harbor, ME) and replaced every 4 generations. Animals were housed on a 12-hour light/dark schedule with ad libitum access to rodent chow and water. All protocols were in accordance with National Institutes of Health guidelines and were approved by the Animal Care and Use Committee at Duquesne University (Pittsburgh, PA; protocol #1407-07 and #1603-03). Experimental sample sizes were determined via power analysis (expected means and SD based on previously published experiments of a similar nature from our own laboratory^{13,37}).

2.2. Urinary bladder distension

Noxious bladder distension produces pain in humans and nociceptive behaviors in rodents.^{31,32} The visceromotor response (VMR) is a spinobulbospinal reflex and quantitative measure of these pain-like responses. The VMRs are obtained by measuring the electrical activity (electromyography [EMG]) of the external oblique abdominal muscle during bladder distension; this EMG is a reliable reproducible measure of nociception that is exacerbated by bladder sensitization and reduced after analgesic administration.³¹ In these experiments, UBD was performed as previously reported.^{13,41,42} Briefly, mice were anesthetized with isoflurane in an induction chamber and then transferred to a nose cone administering 2% isoflurane (vaporized with 100% O₂). An incision was made in the lower skin of the abdomen, and 2 silver wires were implanted in the left abdominal muscle. A third grounding wire was laced through the skin overlying the chest cavity. Lastly, a lubricated 24-gauge 14-mm angiocatheter was inserted in the bladder via the urethra.

After surgical completion, isoflurane was lowered to 1.5% for 10 minutes. Isoflurane was then gradually lowered by an additional 0.125% every 10 minutes until animals responded to noxious toe pinch but were not vocalizing or ambulating (typically 0.8%-0.875%). Once at a stable isoflurane level, animals' bladders were distended 5 times with 60 mm Hg compressed air. Air pressure was controlled by a custom timed-pressure regulator (Washington University School of Medicine Machine Shop, St. Louis, MO). Each distension lasted 20 seconds with a 1-minute intertrial interval. The VMR signal was relayed in real time using a preamplifier (P5 Series, Grass Technologies, West Warwick, RI) via a Cambridge Electronic Design (CED, Cambridge, United Kingdom) module (1401 Plus) to a PC equipped with Spike2 data acquisition software (Version 7, CED). The VMRs were exported to IgorPro 6.22 software (Wave-metrics) where, using a custom script, they were subtracted from background EMG activity, rectified, and integrated over the 20-second distension period. A similar script was used to analyze the EMG activity during the 20-second predistension period. To normalize, all distension VMRs were divided by the smallest predistension VMR for an individual experiment.

Animals exhibiting stable VMRs during initial test distensions were carried throughout the experiment. Distension parameters for individual experiments are described in detail below. For all experiments, animal body temperature was maintained at $37^{\circ}\text{C} \pm 1^{\circ}\text{C}$ using overhead radiant lighting and a battery-operated heating pad. Isoflurane levels were not adjusted once baseline testing started.⁴¹

2.3. Surgical implantation of cannula in the central amygdala

Cannulation of the CeA was performed as previously described.¹³ Briefly, mice were anesthetized in an isoflurane induction chamber and then transferred to a stereotaxic frame (Kopf) fitted with a nose cone administering 2% isoflurane. An 8.0-mm (0.2 mm diameter) stainless steel guide cannula was implanted directly above the left or right CeA (bregma: -1.45 mm, midline: ± 3.0 mm, skull: -4.2 mm) and affixed to the skull using 2 bone screws and dental cement.

2.4. Optogenetic vectors, infusion, stimulation, and protein visualization

2.4.1. Vectors—Yellow fluorescent protein (YFP)-tagged channelrhodopsin-2 (ChR2; rAAV5/EF1 α -DIO-hChR2(H134R)-eYFP) and halorhodopsin (NpHR; rAAV5/EF1 α -DIO-eNpHR3.0-eYFP) constructs and YFP control (rAAV5/EF1 α -DIO-eYFP) construct were obtained from the UNC Vector Core (Chapel Hill, NC).⁵¹ All AAV vectors were driven by the EF1 α promoter and optimized for Cre-mediated recombination via double-floxed inverted orientation (DIO) sequences.

2.4.2. Infusion—Immediately after cannulation surgery described above, nestin-Cre (B6.Cg-Tg(Nes-cre)1Kln/J) female mice aged 9 to 12 weeks received 1 μL injection of appropriate viral vector.⁴⁷ Injections were performed using a 32-gauge injection cannula that extended 0.5 mm beyond the tip of the guide cannula. The injection cannula was coupled to a Hamilton syringe via flexible plastic tubing. One microliter infusion occurred over 5 minutes, and then injector remained in place for 5 additional minutes to allow for virus diffusion. Animals were returned to home cages with an 8.0-mm stylet in cannula to prevent clogging. Optogenetic stimulation and behavioral testing occurred 3 weeks later allowing for optimal viral expression.⁵²

2.4.3. Optogenetic stimulation during urinary bladder distension—An 8.0-mm fiber optic (0.2 mm diameter, Thorlabs, Newton, NJ) connected via FC/PC adaptor to a 473-nm blue or 532-nm green laser diode (Shanghai Laser and Optics Century Co, Ltd, Shanghai, China) was placed in guide cannula immediately after completion of electrode and catheter implantation. Stimulation parameters were similar to previously published studies.^{8,13} For ChR2 activation, 473-nm light was pulsed to mimic CeA firing pattern in rodent neurons after injury (5 ms, 20 Hz, 18 ms spike width pulse train, 8–15 mW power²³). After the completion of baseline UBD testing (5 distensions at 30 mm Hg alternating with 5 distensions at 60 mm Hg), the laser was turned on for 20 minutes and remained on during “laser” time point distensions (same parameters as baseline). After completion of laser distensions, laser was turned off, 15 minutes passed, and “post-laser” distensions (same parameters as baseline) were completed. For NpHR inhibition, 532-nm light (8–12 mW power) was continuously administered for 20 minutes prior to and during laser distensions.⁸

All other timing and distension parameters were identical to ChR2 experiments. Experimenter was blinded to treatment of mouse (ie, YFP vs ChR2/NpHR).

2.4.4. Optogenetic stimulation during abdominal mechanical sensitivity testing—After baseline sensitivity testing in both naive and cyclophosphamide (CYP)-sensitized states (see below), an 8.0-mm fiber optic was placed in each animal's guide cannula. Fibers were connected via FC/PC coupler to a 473-nm blue laser diode. As in UBD experiments, light was pulsed to mimic rodent CeA firing after injury (5 ms, 20 Hz, 18 ms spike width pulse train, 15 mW power). Laser time point testing began as soon as the laser was turned on. Mechanical sensitivities of the left and right sides of the abdomen were assessed twice, with at least 5 minutes passing before retesting on the same side. Once all 4 trials were complete, the laser was turned off and at least 5 minutes passed before post-laser testing was started. Experimenter was blinded to treatment of mouse (ie, YFP vs ChR2).

2.4.5. Yellow fluorescent protein visualization—Since all constructs contained YFP sequence, direct visualization of viral infection was possible. After all optogenetic experiments, animals were injected with Euthazol and then transcardially perfused with phosphate-buffered saline (PBS) (37°C) and 4% paraformaldehyde (PFA, 4°C) in PBS. Brains were removed and stored in 4% PFA overnight at 4°C before being transferred to 20% sucrose. After 24 hours in sucrose, brains were frozen, cut into 30- μ m coronal sections using a cryostat, and stored in 4°C PBS. Sections were mounted onto slides, and YFP targeting was imaged using a Nikon Eclipse E600 epifluorescent microscope. All targeting was done blinded to viral vector treatment. Animals that were off-target were discarded from further data analysis.

2.5. In vivo extracellular verification of optogenetic activation

The ChR2- or NpHR-mediated excitability changes were verified using single-electrode extracellular recordings prior to and during laser stimulation. Optrodes were created as previously described.¹⁸ Single carbon fibers (~8 cm long) coupled to silver wire were epoxied into glass capillary tubes. A micropipette puller (Sutter Instrument Co Model P-97) melted and pulled the capillary tube to a fine point around the fiber. Fiber tips were burned down until ~5 μ m remained outside of the capillary glass. Polished fiber optics were coupled to electrodes, ensuring that the 2 tips were less than 200 μ m apart.

The electrode was connected to a signal amplifier (WPI, ISO-80) with a voltage gain of $\times 10^3$ and integrated low- and high-pass filters set to 300 Hz and 3.0 kHz, respectively. This was then placed in series to a HumBug 60-Hz noise filter (Quest Scientific, North Vancouver, Canada). The filtered signal was processed by an analog/digital converter (Cambridge Electronic Design Ltd, Micro 1401-3) and the Spike2 software (CED). Filtered noise levels were typically <0.05 mV.

Animals received 1 μ L injections of ChR2 or NpHR in the CeA as described above. Three weeks after injection, animals were placed into a stereotaxic frame administering 2% isoflurane. The skull overlying the CeA coordinates (see above) was removed, and 0.5% agar was placed over the brain to prevent drying of the tissue. Using a stereotaxic

micropositioner, the optrode was lowered 3200 μm and then in 5- μm bursts until single-unit spikes were identified.

Action potentials were counted immediately before and during laser stimulation by a custom script in the Spike2 software using the WaveMark feature. Firing frequencies were averaged for each interval. The location of each recording was marked by driving current through the electrode via the WPI ISO-80. Featured data represent multiple trials of neurons in 2 Chr2-injected and 2 NpHR-injected mice. The brain was removed, fixed in 4% PFA overnight, cryopreserved in 20% sucrose, and then cut into 35- μm coronal sections. Mounted sections were stained with hematoxylin (15 minutes) and eosin (5 seconds), and then lesions were identified using a Nikon Eclipse E600 light microscope.

2.6. Immunohistochemistry

2.6.1. NeuN density in left/right central amygdala—Naive C57Bl/6 mice were euthanized, and brains were fixed and sectioned as described above. Sections spanning the rostral–caudal extent of the CeA were blocked in 50% Odyssey blocking buffer and 0.3% Triton X-100 in PBS for 1 hour and then incubated with mouse anti-NeuN primary antibody (1:200, Millipore Cat# MAB377 RRID:AB_2298772; in 30% Odyssey blocking buffer, 0.3% Triton X-100 in PBS) overnight at 4°C. Sections were washed in PBS and then incubated with goat anti-mouse Alexa 680 secondary antibody (1:5000, Molecular Probes, Eugene, OR; in 30% Odyssey blocking buffer, 0.3% Triton X-100 in PBS) for 1 hour. After a final PBS wash, sections were slide mounted and then visualized using an Odyssey Imaging System (LI-COR). Using the Paxinos and Franklin Brain Atlas as a guide, freehand shapes around the left and right CeA were drawn in Image Studio Lite software (version 4.0, LI-COR) and signal/area values for each nucleus were calculated in a blinded fashion.³⁸

2.6.2. cFos staining in the left/right central amygdala and parabrachial nucleus after bladder distension—After completion of UBD, animals were injected with Euthasol and brains removed and processed as described above; for PBn cFos experiments, sham animals were catheterized but did not have bladders distended. Ten CeA or PBn sections identified using the Paxinos and Franklin Brain Atlas were incubated in 1% H₂O₂ in PBS for 5 minutes, rinsed with PBS, and then blocked in 10% normal goat serum (NGS) and 0.1% Triton X-100 in PBS for 1 hour. Sections were incubated with rabbit anti-cFos primary antibody (1:20,000, Millipore Cat #ABE457; in 3% NGS, 0.1% Triton X-100 in PBS) overnight at 4°C. After PBS wash, sections were incubated with goat anti-rabbit biotinylated immunoglobulin G (1:200, Vector; in 1% NGS in PBS) for 1 hour. Sections were rinsed with PBS, incubated in Vectastain ABC solution (Vector) for 1 hour, washed with PBS again, and then placed in DAB substrate working solution (Vector) for 60 seconds. After a final rinse in PBS, sections were mounted, coverslipped, and viewed using a Nikon Eclipse E600 light microscope. After delineating the CeA or PBn, cFos-positive cells were counted and averaged across sections for each animal using ImageJ software by an experimenter blinded to treatment and side of brain.

2.6.3. Hematoxylin and eosin staining of bladder tissue—Bladders from CYP- and saline-treated mice were dissected after behavioral testing and fixed in 4% PFA for 24 hours.

Bladders were cryopreserved in 20% sucrose for an additional 24 hours and then cut into 30- μ m cross sections. Slide-mounted sections were stained in 0.1% hematoxylin for 4 minutes, rinsed in tap water for 5 minutes, and then destained in 10% acetic acid in 95% ethanol for 1 minute. After a 1-minute tap water rinse, sections were stained in 0.5% eosin for 2 minutes and then put through a final rinse. Sections were viewed using a Nikon Eclipse E600 light microscope.

2.7. Pituitary adenylate cyclase–activating polypeptide administration and effects on urinary bladder distension

At least 5 days after CeA cannulation procedure, animals underwent catheterization and electrode implantation for UBD (see above). For baseline VMR recording, bladders were distended in triplicate at 15, 30, 45, 60, and 75 mm Hg (20 seconds distension, 1 minute intertrial interval). Immediately after completion of final 75 mm Hg distension, animals received 0.5 μ L injection of 1 μ g/ μ L or 10 μ g/ μ L PACAP-38 solution (Sigma) or 0.05% bovine serum albumin in saline vehicle through left/right CeA cannula. These doses were adapted from those that produced nociceptive effects in rat.²⁸ Injections were performed using a 32-gauge injection cannula that extended 0.5 mm beyond the tip of the guide cannula. The injection cannula was coupled to a Hamilton syringe via flexible plastic tubing. Infusion occurred over 3 minutes, and then injector remained in place for 2 additional minutes to allow for diffusion. Thirty and 60 minutes after infusion start, bladders were distended similar to baseline recordings. At the end of each experiment, animals were euthanized and their brains removed and sectioned to determine proper cannula targeting. Experimenter was blinded to treatment until after cannula targeting verification.

2.8. Abdominal mechanical sensitivity testing

Two days prior to testing, animals were anesthetized with 2% isoflurane and all hair from the abdominal area was removed with electric clippers. On testing day, animals habituated for 1.5 hours in 10 cm² \times 15 cm high plexiglass enclosures; low-decibel white noise was used to mitigate background sounds. The experimenter was present in the room for 30 minutes prior to start of testing to eliminate any sex-induced analgesic effects.⁴⁴ Using calibrated von Frey filaments (0.02–2.56 g) and the up–down assessment method, withdrawal thresholds were measured for the left and right sides of the abdomen approximately 0.5 cm away from the urethra.¹¹ Beginning with 0.32 g, filaments were applied to the testing site until bent at 30° for approximately 2 seconds. If an animal withdrew from the stimulus, the next smallest filament was applied; if there was no response to stimulation, the next largest filament was applied. Stepwise increasing or decreasing stimulation was performed until there was a change in response (ie, no response followed by response or vice versa). After this change, 4 more stimulations were completed in the up–down fashion and 50% withdrawal thresholds were calculated as previously reported.¹⁷ Each side of the abdomen was tested twice, waiting 5 minutes between trials. All 4 withdrawal thresholds (2/side/trial) were averaged together to obtain an average 50% withdrawal threshold for each animal. Experimenter was blinded to ChR2 vs YFP and CYP vs saline treatment.

2.9. Cyclophosphamide-induced bladder sensitization

Cyclophosphamide is a chemotherapeutic drug that when metabolized breaks down into cystitis-inducing chemical acrolein.⁴⁵ In these studies, animals received 100 μ L intraperitoneal injections of 100 mg/kg CYP (Sigma) or saline vehicle every other day for 5 days prior to UBD or behavioral testing (ie, injections occurred on days 1, 3, and 5 and then UBD or von Frey was performed on day 6). Cyclophosphamide was made fresh each day, immediately prior to injection.

2.10. Data analysis

Prism 5 software (GraphPad) was used to analyze all data. Results are expressed as means \pm SEM. Student *t* tests were used to compare 2 means. Two-way analysis of variance (ANOVA) with repeated measures (RM) was used to analyze data sets containing 2 independent variables; Bonferroni post hoc tests were employed when significant main effects were found. A value of $P < 0.05$ was considered statistically significant for all comparisons.

3. Results

3.1. Optogenetic activation of the right central amygdala increases pain-like responses to noxious bladder distension

To dissect the functional contributions of the left and right CeA in bladder pain processing, we used optogenetics to independently activate each nucleus during noxious UBD. In these experiments, AAV vectors containing either double-floxed YFP-tagged ChR2 or double-floxed control YFP (YFP) were stereotaxically targeted to the left or right CeA of mice expressing Cre recombinase under the nestin promoter.^{13,26} ChR2 functionality was verified using in vivo extracellular recording; firing rates of neurons in ChR2-expressing areas of the CeA significantly increased during 473-nm, 20-Hz light stimulation (Fig. 1A; paired *t* test $t[8] = 5.105$, $P = 0.0009$, $n = 9$). Following Cre-mediated recombination, YFP was broadly observed throughout the CeA in each of the experimental (left ChR2, right ChR2) and control groups (left YFP, right YFP) (Fig. 1B).

Visceromotor responses to noxious bladder distension (60 mm Hg pressure) were recorded in each animal prior to (baseline), during (laser), and after (post-laser) laser stimulation to determine the effects of global activation of the left or right CeA on bladder pain modulation (Fig. 1C – E). Increased responses to noxious bladder distension were observed during optical stimulation of ChR2-expressing right CeA (Fig. 1D, E; 2-way RM ANOVA significant main effect of group $F_{3,71} = 3.668$, $P = 0.0296$; main effect of time $F_{2,71} = 3.720$, $P = 0.0330$; main effect of interaction $F_{6,71} = 6.254$, $P = 0.0001$; $n = 6$; Bonferroni posttest right ChR2 vs right YFP at laser, *** $P < 0.001$, right ChR2 vs left ChR2 at laser, *** $P < 0.001$, right ChR2 laser vs baseline, *** $P < 0.001$). These increases in nociception were specific to distension intervals and not a result of increased background EMG signals. Central amygdala activation did not induce nonspecific abdominal contraction between distension trials (average EMG [V] for 20 seconds pre-pressure interval for left YFP at baseline: 0.202 ± 0.004 , at laser: 0.204 ± 0.005 ; right YFP at baseline: 0.229 ± 0.013 , at laser: 0.231 ± 0.014 ; left ChR2 at baseline: 0.227 ± 0.013 , at laser: 0.318 ± 0.081 ; right

ChR2 at baseline: 0.231 ± 0.022 , at laser: 0.239 ± 0.023 ; 2-way RM ANOVA no main effect of time $F_{1,47} = 1.601$, $P = 0.2203$; no main effect of group $F_{3,47} = 1.346$, $P = 0.2876$; no main effect of interaction $F_{3,47} = 1.138$, $P = 0.3576$; $n = 6$).

Optical stimulation in animals expressing ChR2 in the left CeA did not significantly increase bladder pain-like responses (Fig. 1C, E). After laser cessation, pain-like responses were similar across groups and were not significantly different from baseline responses. When the left or right CeA expressed only YFP, optical stimulation had no effect on bladder pain-like responses (Fig. 1E). Overall, these data suggest asymmetrical modulation of noxious bladder signaling by the left and right CeA.

3.2. Left and right central amygdalae do not differ in neuron number or activation levels as measured by cFos expression during channelrhodopsin-2-mediated depolarization

Two potential explanations for the asymmetric physiological responses reported during left/right CeA activation are differences in neuron number and experiment-induced cellular activation levels within each nucleus. First, to determine if there are intrinsic differences in the number of neurons within the left and right CeA, brain sections spanning the rostrocaudal extent of the CeA were stained for NeuN, a neuron-specific nuclear protein. In naive female C57Bl/6 mice, the background strain for animals used in the optogenetic experiments, no statistically significant differences in NeuN signal were detected between the left and right CeA (Fig. 2A; paired t test $t_{(7)} = 0.2311$, $P = 0.8238$; $n = 8$).

Next to determine if these symmetric populations of neurons were equally activated during optical excitation and noxious bladder distension, we performed cFos immunohistochemistry on brain sections covering the rostrocaudal extent of the CeA centered on the resting location of the fiber optic. cFos-positive cells were counted in both the injected (ie, cannula implanted, virus infected, and laser stimulated) and noninjected (ie, naive) CeA of individual mice for the left and right ChR2-expressing groups (Fig. 2B) and YFP-only-expressing nuclei (Fig. 2C). Both left and right ChR2-expressing nuclei contained more cFos-positive cells than respective noninjected nuclei (Fig. 2D; 2-way RM ANOVA main effect of injection $F_{1,47} = 50.20$, $P < 0.0001$; main effect of interaction $F_{2,47} = 5.227$, $P = 0.0144$; no main effect of group $F_{2,47} = 1.248$, $P = 0.3075$; $n = 6-11$; Bonferroni posttest for left ChR2 injected vs left noninjected, $***P < 0.001$, right ChR2 injected vs right noninjected, $**P < 0.01$); however, there was no difference in cFos expression between left and right ChR2-injected nuclei (Bonferroni posttest for left ChR2 injected vs right ChR2 injected, $P > 0.05$). Similarly, there was no difference in cFos expression between the noninjected left and right CeA (Bonferroni posttest for left ChR2 noninjected vs right ChR2 noninjected, $P > 0.05$). A nonsignificant trend toward increased cFos expression was observed in YFP-injected nuclei when compared with noninjected nuclei, most likely due to viral transduction or mechanical stimulation during fiber optic insertion.

3.3. Central amygdala afferents differentially contribute to noxious bladder sensation

The left and right CeA are heterogeneous nuclei, containing diversely labeled afferent terminals, interneurons, and efferent cell bodies. The 2 primary sites from which CeA afferent terminals arise are the PBn and basolateral amygdala (BLA), each signaling through

unique neurotransmitter systems. Here, we assessed unilateral functional contributions of the PBN and BLA to nociceptive bladder transmission in the CeA using pharmacological means or optogenetics in conjunction with UBD.

To model PBN signaling, PACAP was unilaterally injected in the left or right CeA. Pituitary adenylate cyclase-activating poly-peptide is a widely distributed pleiotropic peptide, but detection of this molecule in the CeA is largely limited to release from PBN projection neurons; BLA terminals within the CeA do not release PACAP.^{28,49} Responses to innocuous and noxious bladder distension were measured from left abdominal muscles prior to PACAP infusion (baseline) and then 30 and 60 minutes after PACAP infusion. First, 0.5 μ g of PACAP was infused into the left (Fig. 3A) or right CeA (Fig. 3B).²⁸ When applied to the left CeA, this dose of PACAP had no effect on the graded responses generated by increasing pressure within the bladder (Fig. 3A; 2-way RM ANOVA no main effect of treatment $F_{2,119} = 1.268$, $P = 0.2878$; main effect of pressure $F_{4,119} = 4.652$, $P = 0.0041$; no main effect of interaction $F_{8,119} = 0.9080$, $P = 0.5151$; $n = 8$). Conversely, application of 0.5 μ g of PACAP in the right CeA significantly increased responses to graded UBD for at least 60 minutes after PACAP infusion (Fig. 3B; 2-way RM ANOVA main effect of treatment $F_{2,119} = 6.723$, $P = 0.0021$; main effect of pressure $F_{4,119} = 3.280$, $P = 0.0220$; no main effect of interaction $F_{8,119} = 0.1427$, $P = 0.9968$; $n = 8$).

A second 10-fold higher dose of PACAP (5 μ g) was next infused into the left (Fig. 3C) or right CeA (Fig. 3D) to ensure that the lack of effect observed with 0.5 μ g PACAP in the left CeA was not a consequence of underdosing. As with 0.5 μ g PACAP, 5 μ g PACAP application in the left CeA failed to significantly change responses to graded UBD (Fig. 3C; 2-way RM ANOVA no main effect of treatment $F_{2,50} = 0.3709$, $P = 0.6924$; main effect of pressure $F_{4,50} = 14.84$, $P < 0.0001$; no main effect of interaction $F_{8,50} = 0.6389$, $P = 0.7413$; $n = 6$). Application of 5 μ g PACAP in the right CeA, however, significantly increased responses to graded UBD just as the 0.5 μ g dose had (Fig. 3D; 2-way ANOVA main effect of treatment $F_{2,50} = 15.90$, $P < 0.0001$; no main effect of pressure $F_{4,50} = 2.402$, $P = 0.0767$; no main effect of interaction $F_{8,50} = 1.229$, $P = 0.3022$; $n = 6$). Significant increases in pain-like responses were observed at the most noxious pressures 30 and 60 minutes after PACAP administration (Bonferroni posttest for baseline vs 30 minutes, $*P < 0.05$ at 75 mm Hg, for baseline vs 60 minutes, $**P < 0.01$ at 60 and 75 mm Hg).

To address the lateralized nature of UBD (ie, EMG recording can only be completed on one side of the body) and potential contralateral nociceptive modulation by PACAP, the above experiment was repeated in a separate cohort of animals, recording VMRs from the right abdominal muscle instead of the left. Application of 5 μ g of PACAP in the left CeA did not change UBD-evoked VMRs recorded from the right abdominal muscle (Fig. 3E; 2-way RM ANOVA no main effect of treatment $F_{2,50} = 1.465$, $P = 0.2407$; no main effect of pressure $F_{4,50} = 1.164$, $P = 0.3505$; no main effect of interaction $F_{8,50} = 0.5408$, $P = 0.8201$; $n = 6$). However, similar to what was observed during left abdominal recording, statistically significant increases in UBD-evoked VMRs were recorded from the right abdominal muscle after 5 μ g PACAP application in the right CeA (Fig. 3F; 2-way RM ANOVA main effect of treatment $F_{2,50} = 12.90$, $P < 0.0001$; no main effect of pressure $F_{4,50} = 2.080$, $P = 0.1136$; no

main effect of interaction $F_{8,50} = 0.8463$, $P = 0.5670$; $n = 6$; Bonferroni posttest for baseline vs 30 minutes, $*P < 0.05$ at 60 and 75 mm Hg).

To maintain experimenter blinding, all PACAP-injected animals were concurrently tested with vehicle-treated mice (Fig. 3G, H). As expected, vehicle application in neither the left (Fig. 3G; 2-way RM ANOVA no main effect of treatment $F_{2,120} = 1.321$, $P = 0.2818$; main effect of pressure $F_{4,120} = 6.275$, $P = 0.0001$; no main effect of interaction $F_{8,120} = 0.7946$, $P = 0.6084$; $n = 11$) nor the right CeA (Fig. 3H; 2-way RM ANOVA no main effect of treatment $F_{2,108} = 0.9577$, $P = 0.3964$; main effect of pressure $F_{4,108} = 4.191$, $P = 0.0034$; no main effect of interaction $F_{8,108} = 1.191$, $P = 0.3110$; $n = 10$) significantly changed VMRs during graded UBD.

To evaluate whether baseline UBD might be differentially activating the left and right PBn and thus causing unequal endogenous release of PACAP in the CeA at later time points, PBn activation was measured via cFos expression after one round of graded UBD (Fig. 4A). Urinary bladder distension significantly increased cFos expression to a similar extent in both the left and right PBn compared with sham control animals (Fig. 4B; 2-way RM ANOVA main effect of UBD $F_{1,23} = 17.84$, $P = 0.0018$; no main effect of side of brain $F_{1,23} = 0.1588$, $P = 0.6986$; no main effect of interaction $F_{1,23} = 0.4474$, $P = 0.5187$; $n = 6$; Bonferroni posttest for UBD left PBn vs right PBn, $P > 0.05$; left PBn sham vs UBD, $*P < 0.05$; right PBn sham vs UBD, $**P < 0.01$). Although these data do not specifically measure UBD-evoked PACAP release in the CeA, it should be noted that cFos-positive cell populations were only observed in the lateral PBn, the subdivision in which PACAP CeA projection neuron cell bodies reside (Fig. 4A).²⁸

Left and right BLA contributions to bladder pain processing were explored using excitatory optogenetic approaches and UBD. Basolateral amygdala projections to the CeA are primarily glutamatergic; due to the ubiquitous nature of glutamate within the CeA, direct administration of this neurotransmitter would not accurately mimic BLA signaling as PACAP administration had done for PBn transmission.^{43,48} No significant change in VMRs was observed after ChR2-mediated activation of either the left or right BLA (normalized VMRs [Vs] for left BLA-ChR2 at baseline: 4.21 ± 0.47 , at laser: 3.38 ± 0.69 , at post-laser: 3.23 ± 0.86 ; for right BLA-ChR2 at baseline: 3.59 ± 0.37 , at laser: 2.73 ± 0.34 , at post-laser: 2.80 ± 0.51 ; 2-way RM ANOVA no main effect of time $F_{2,47} = 2.316$, $P = 0.1173$; no main effect of side of brain $F_{1,47} = 0.8706$, $P = 0.3666$; no main effect of interaction $F_{2,47} = 0.03266$, $P = 0.9679$; $n = 8$). Combined, these data discriminate contributions of the PBn and BLA to nociceptive bladder transmission in the CeA.

3.4. Optogenetic inhibition of the left central amygdala increases pain-like responses to noxious bladder distension

Global activation of the left and right CeA resulted in asymmetric physiological responses, ultimately suggesting a pronociceptive output from the right CeA and leaving the functional contributions of the left CeA unclear. To better understand the intrinsic functions of the left and right CeA during instances of bladder pain, and not just what occurs during exogenous optogenetic activation, we optically inhibited each nucleus during noxious bladder distension. AAV vectors containing double-floxed YFP-tagged halorhodopsin (NpHR) or

double-floxed YFP alone (YFP) were injected into the left and right CeA of nestin-Cre animals. NpHR in vivo functionality was verified similar to ChR2; firing rates of neurons in NpHR-expressing regions of the CeA significantly decreased during 532-nm light stimulation (Fig. 5A; paired t test $t [4] = 3.620$, $P = 0.0224$; $n = 5$). Cre-mediated expression of YFP was observed in each of the experimental (left NpHR, right NpHR) and control groups (left YFP, right YFP) (Fig. 5B).

Animals were then placed through 3 sets of noxious bladder distension to obtain pain-like responses before (baseline), during (laser), and after (post-laser) global optical inhibition of each nucleus. NpHR-mediated hyperpolarization in the right CeA had no effect on bladder pain-like responses (Fig. 5D, E). Additionally, light stimulation in YFP-only control animals had no effect on bladder nociception; since right YFP and left YFP groups were not statistically or functionally different from one another in previous UBD experiments (Fig. 1E), groups were combined for this and all additional optogenetic analyses. Optical inhibition of the left CeA increased pain-like responses during noxious bladder distension (Fig. 5C, E; 2-way RM ANOVA main effect of interaction $F_{4,104} = 3.776$, $P = 0.0081$; no main effect of time $F_{2,104} = 0.3664$, $P = 0.7156$; no main effect of group $F_{2,104} = 0.6890$, $P = 0.5094$; $n = 9-17$; Bonferroni posttest left NpHR vs right NpHR at laser, $*P < 0.05$; left NpHR vs YFP at laser, $*P < 0.05$; left NpHR laser vs baseline, $*P < 0.05$). These data suggest an ongoing antinociceptive output from the left CeA.

3.5. Following bladder inflammation, left and right central amygdalae have opposing nociceptive functions

Injury state is known to affect background and nociceptive-specific activities in the CeA.²³ To determine if bladder inflammation alters the magnitude or functional nociceptive properties of left or right CeA activity, excitatory optogenetics were again employed during UBD after bladder sensitization. Cyclophosphamide, an alkylating antineoplastic drug, was systemically administered to animals at a dose (100 mg/kg) and schedule (every other day for 5 days) previously reported to increase UBD-evoked VMRs.¹⁵ Twenty-four hours after the final CYP injection, UBD-evoked VMRs were recorded prior to (baseline), during (laser), and after completion of (post-laser) ChR2-mediated activation of the left (Fig. 6A) or right CeA (Fig. 6B). Similar to naive animals (Fig. 1D, E), bladder-sensitized animals also exhibited significant increases in UBD-evoked VMRs during optogenetic activation of the right CeA (Fig. 6B, C; 2-way RM ANOVA main effect of group $F_{2,28} = 5.088$, $P = 0.0218$; no main effect of time $F_{2,28} = 2.077$, $P = 0.1442$; main effect of interaction $F_{4,28} = 3.242$, $P = 0.0264$; $n = 5-7$; Bonferroni posttest right ChR2 vs YFP at laser, $**P < 0.01$; right ChR2 baseline vs laser, $*P < 0.05$). This increase in VMR was significantly different from the slight nonstatistically significant decrease in VMR observed during optogenetic activation of the left CeA (Fig. 6A, C; Bonferroni posttest right ChR2 vs left ChR2 at laser, $***P < 0.001$). Laser stimulation in YFP-expressing control mice had no effect on UBD-evoked VMRs, as expected.

After this assessment in lightly anesthetized animals, we also examined the capacity of the left and right CeA to modulate referred bladder pain in awake-behaving animals. Referred pain is a phenomenon in which visceral discomfort manifests in a nearby somatic structure

as a result of overlapping primary afferent termination on second-order neurons within the spinal cord. In these experiments, referred pain-like symptoms were induced using CYP and assessed on the abdominal surface immediately external to the bladder. Abdominal mechanical sensitivity was assessed prior to and 24 hours after a 5-day CYP or vehicle treatment schedule (injections on days 1, 3, and 5; behavioral testing on day 6) using calibrated von Frey filaments. Similar to previous reports,⁶ CYP-treated animals developed robust mechanical hypersensitivity after 5 days of treatment while saline controls had no significant change in abdominal sensitivity (Fig. 7A; 2-way RM ANOVA main effect of CYP $F_{1,47} = 10.18$, $P = 0.0042$; main effect of interaction $F_{1,47} = 11.15$, $P = 0.0030$; no main effect of time $F_{1,47} = 1.372$, $P = 0.2541$; $n = 12$; Bonferroni posttest CYP vs saline at postinjection, *** $P < 0.001$). Additionally, CYP-treated mice displayed noticeable qualitative changes in bladder morphology, including thickening of the urothelium and edema throughout the submucosa, indicative of an ongoing inflammatory response¹⁵ (Fig. 7B).

Using this model and ChR2-driven optogenetics, we were next able to delineate the functions of the left and right CeA in the modulation of abdominal mechanical sensitivity in both naive and injured states. As before, YFP-tagged ChR2 and YFP alone were broadly observed throughout the CeA in the experimental (left ChR2, right ChR2) and control groups (YFP), respectively (Fig. 7C). Three weeks after CeA cannulation and viral injection, abdominal sensitivity was assessed prior to (baseline), during (laser), and after (post-laser) ChR2-mediated activation of the left or right CeA. Under naive conditions, activation of the right and left CeA had opposite effects on abdominal sensitivity; activation of the right CeA significantly increased abdominal sensitivity (ie, decreased withdrawal thresholds) while activation of the left CeA trended toward decreased mechanical sensitivity (ie, increased withdrawal thresholds) (Fig. 7D; 2-way ANOVA main effect of group $F_{2,146} = 6.673$, $P = 0.0017$; main effect of time $F_{5,146} = 20.51$, $P < 0.0001$; no main effect of interaction $F_{10,146} = 1.803$, $P = 0.0661$; $n = 7-10$; Bonferroni posttest right ChR2 vs left ChR2 at naive laser, * $P < 0.05$). As expected, laser stimulation of YFP-only-expressing CeA did not change abdominal withdrawal thresholds.

After assessments in the naive state, all animals were treated with CYP. All groups exhibited referred bladder pain as evidenced by decreased withdrawal thresholds during CYP baseline mechanical testing (Fig. 7D; Bonferroni posttest naive baseline vs CYP baseline for YFP, $P < 0.0001$; for left ChR2, $P < 0.05$; for right ChR2, $P < 0.01$). Laser stimulation of YFP-only-expressing CeA had no effect on abdominal sensitivity as expected. Similarly, no effect of right CeA activation was observed although this was likely due to a floor effect in the assay (ie, animals responded to all filaments and could not show additional hypersensitivity). Activation of the left CeA following inflammation, however, completely reversed CYP-induced referred bladder pain, increasing withdrawal thresholds to pre-inflammation levels (Fig. 7D; Bonferroni posttest left ChR2 vs right ChR2 at CYP laser, * $P < 0.05$; CYP laser vs naive baseline for left ChR2, $P = 0.9908$).

4. Discussion

Prior to these studies, the function of the left CeA in visceral pain processing was unknown. Here, we observed an ongoing antinociceptive output of this nucleus in 2 different bladder pain assays. Using excitatory optogenetics, we also established the pronociceptive function of the right CeA in the context of noxious bladder distension and extended this property to abdominal mechanical sensation in awake-behaving animals. These data suggest functional lateralization of CeA activity during visceral pain modulation in rodents. To our knowledge, only one other report has investigated amygdala lateralization in rodent visceral pain; unilateral corticosterone application to the left or right CeA failed to increase rectal pain measures but was sufficient to increase anxiety behaviors.⁴⁶ In contradiction with our studies, these results may be due to the activating stimulus (ie, light vs hormone) or the population of cells activated by each manipulation (ie, all neurons vs only those expressing glucocorticoid receptors).

Functional cerebral lateralization is a neurological phenomenon present throughout the vertebrate phylogenetic tree. Hemisphere-specific communication processing centers, like Broca's and Wernicke's areas in humans and the left pretrigeminal area of frogs, are thought to have evolved as a way to reduce neural circuit complexity, redundancy, and functional interference.^{4,20} In addition to these regions, lateralization of the amygdala has been documented during complex behaviors, including emotional processing and memory consolidation.^{2,12} Recent studies generated by the Multidisciplinary Approach to the Study of Chronic Pelvic Pain network have also demonstrated unilateral changes in the amygdala of patients with chronic bladder pain. Patients with interstitial cystitis/bladder pain syndrome exhibit increases in gray matter and functional connectivity of the left amygdala at rest, and during bladder stimulation, right amygdala functional connectivity is altered compared with healthy controls.^{1,3,24,27}

Our data suggest a pronociceptive function for the right CeA. Related experiments demonstrate similar lateralization in somatic pain. Right lateralized phosphorylation of extracellular signal-regulated kinase 2 is observed 3 hours into ongoing peripheral inflammation while phosphorylated extracellular signal-regulated kinase 2 increases are not observed in the left CeA at any time during inflammation.⁹ Similarly, 5 hours after experimental induction of arthritis, increased baseline and evoked activities are observed only in right CeA neurons.²³ In a more chronic example, increased evoked activity is observed in the right CeA 14 days after spinal nerve ligation surgery.²¹ Collectively, these data suggest preferential recruitment of the right CeA during acute and persistent pain. Recruitment of this pronociceptive nucleus may then continue to drive pain-like behaviors, potentially leading to chronic pain in the absence of peripheral injury.

In the present study, optogenetic inhibition of the right CeA did not decrease VMRs. These data challenge previous experiments from our laboratory in which pharmacological inhibition of mGluR5 in the right CeA decreased bladder pain-like responses.¹³ The mechanism for these discrepancies most likely lies in the technical applications of each manipulation. Due to the generic nature of the nestin promoter, fibers of passage, some potentially involved in antinociceptive circuitry, may have been inhibited during the current

optogenetic experiments in addition to pronociceptive right CeA neurons. Alternatively, antagonist administration may have inhibited activity in mGluR5-expressing amygdaloid glia that may have pronociceptive functions.⁴⁰

The identification of PACAP as a contributor to right CeA pronociceptive tone is important for understanding broader bladder pain circuitry. Chemical sensitization of the bladder increases PACAP expression in the CeA; original reports did not specify if this quantification occurred in a unilateral or bilateral manner.⁵ The main source of PACAP in the CeA is PBn afferent terminals.²⁸ Knowing this, we modeled unilateral PBn activity by administering multiple doses of PACAP in each CeA. Increases in bladder nociception were primarily observed when this peptide was administered in the right CeA and not the left. Future studies should investigate long-term changes in both PBn and CeA PACAP expression in clinical bladder pain populations to determine if this peptide might be a potential therapeutic target.

The functional implications of CeA PACAP administration also help to delineate which CeA afferents are important for bladder pain transmission. The lack of VMR change observed during optogenetic activation of the left or right BLA suggests that bladder pain is preferentially relayed through PBn-CeA synapses and not BLA-CeA connections. This transmission selectivity is further supported by previous studies in which zymosan-induced colitis, another form of visceral pain, enhanced synaptic transmission between the PBn and CeA, but not between the BLA and CeA.²²

Here, we identified antinociceptive functions of the left CeA in both anesthetized and awake measures of bladder nociception; the magnitude of the antinociceptive effect differed between measures, most likely due to anesthetized state or stimulus modality. We predict that the divergent nociceptive circuits of the right and left CeA are engaged at different times throughout the development and maintenance of persistent pain. For instance, the antinociceptive circuits in the left hemisphere are most likely recruited shortly after injury to stabilize and guard against further insult but, after prolonged nociceptive peripheral input, are overwhelmed by the pronociceptive output from the right CeA. Supporting this proposed schedule is the unilateral activation of the left CeA that is reported in both injured rodents and humans. During rectal distension, female patients with irritable bowel syndrome demonstrate left amygdala activation as measured by positron emission tomography scans, and for the first 6 days after spinal nerve ligation, rats display increased evoked nocifensive activity in the left CeA; consistent right CeA increases are not observed until 14 days after surgery.^{21,29}

The mechanisms responsible for left hemisphere antinociceptive effects remain unknown; however, they are most likely a complex blend of anatomical, molecular, and physiological differences. Anatomically speaking, the bladders of male rats are symmetrically innervated by primary afferents that synapse uniformly on both the left and right sides of the spinal cord.^{10,36} Although these studies have not been replicated in female mice, it is logical to assume the same pattern exists across species and sex. After this initial relay, very few projections have been studied in a symmetrical fashion. It is unclear if the left and right CeA receive equal input from spinothalamic tract projecting BLA neurons, spinoparabrachial

tract neurons, or direct projections from second-order neurons located in lamina \times of the spinal cord.³⁰ Our analyses, however, show that bladder distension does induce similar activation of the lateral PBN, suggesting that second order neurons projecting from the spinal cord to the PBN are likely symmetric. Little is known about the efferent anatomical and functional connectivity of the left and right CeA. Only one study has investigated projections from the nociceptive region of the CeA (CeLC), and this study focused solely on projections in the right hemisphere.⁷ Since the CeA projects directly to the periaqueductal gray and indirectly to the rostral ventromedial medulla, 2 key members of the descending nociceptive network, it would not be surprising if asymmetries in these circuits were partially responsible for the divergent phenotypes observed after left and right CeA activation.^{19,39}

In these studies, we provide basic immunohistochemical data to suggest that neuron density in the left and right CeA does not differ; however, we are just beginning to understand the molecular and physiological differences that exist between these similarly sized cell populations. Since we did not use cell type-specific optogenetic techniques in these experiments, it remains to be seen if different cell populations in the left and right CeA mediate the observed divergent physiological effects. Cells in the CeA release a heterogeneous mix of neurotransmitters and express the corresponding receptors, but very few studies have explored relative quantities of these molecules in a symmetric way. In one exception, mGluR5 expression in naive animals was higher in the right CeA than the left³⁷; all other studies reporting CeA protein expression do so in a bilateral fashion or report values for a single side only. Electrophysiological studies have uncovered details on individual nucleus background and stimulus-evoked activities as reported above, but most of these studies have focused on neurons activated by pain. In other words, the background and stimulus-dependent activities in pain-inhibited CeA neurons are relatively unknown.

Overall, these data suggest unique nociceptive properties of the left and right CeA in the context of visceral pain; specifically, the right CeA is pronociceptive and the left CeA is antinociceptive. Furthermore, these reports highlight differences in somatic and visceral nociceptive lateralization in the CeA, beyond that established by peripheral neuroanatomy. While these experiments were completed in naive mice or those experiencing acute bladder sensitization, the unique nociceptive roles of the left and right CeA discovered within begin to provide a basis for understanding the consequences of left and right hemispheric lateralization in patients with chronic pain. Continued exploration into the anatomical, molecular, and physiological explanations for observed asymmetries will hopefully uncover novel therapeutic targets for those suffering from chronic bladder pain conditions.

Acknowledgments

The authors thank Dr Rehanna Leak and laboratory for experimental assistance and equipment access and Bharaniabirami Rajaram, Melissa Wolz, Youstina Seliman, and Caela Long for experimental assistance.

This work was supported by funding from the National Institutes of Health (NIDDK F31DK104538 to K.E.S., NICCIH R15AT008060 to B.J.K.) and the International Association for the Study of Pain (Early Career Research Grant by the Scan/Design Foundation BY INGUR & JENS BRUUN to B.J.K.).

References

1. As-Sanie S, Harris RE, Napadow V, Kim J, Neshewat G, Kairys A, Williams D, Clauw DJ, Schmidt-Wilcke T. Changes in regional gray matter volume in women with chronic pelvic pain: a voxel-based morphometry study. *PAIN*. 2012; 153:1006–14. [PubMed: 22387096]
2. Baas D, Aleman A, Kahn RS. Lateralization of amygdala activation: a systematic review of functional neuroimaging studies. *Brain Res Brain Res Rev*. 2004; 45:96–103. [PubMed: 15145620]
3. Bagarinao E, Johnson KA, Martucci KT, Ichescio E, Farmer MA, Labus J, Ness TJ, Harris R, Deutsch G, Apkarian AV, Mayer EA, Clauw DJ, Mackey S. Preliminary structural MRI based brain classification of chronic pelvic pain: a MAPP network study. *PAIN*. 2014; 155:2502–9. [PubMed: 25242566]
4. Bauer RH. Lateralization of neural control for vocalization by the frog (*Rana pipiens*). *Psychobiology*. 1993; 21:243–8.
5. Bon K, Lanteri-Minet M, Michiels JF, Menetrey D. Cyclophosphamide cystitis as a model of visceral pain in rats: a c-fos and Krox-24 study at telencephalic levels, with a note on pituitary adenylate cyclase activating polypeptide (PACAP). *Exp Brain Res*. 1998; 122:165–74. [PubMed: 9776515]
6. Boudes M, Uvin P, Kerselaers S, Vennekens R, Voets T, De Ridder D. Functional characterization of a chronic cyclophosphamide-induced overactive bladder model in mice. *NeuroUrol Urodyn*. 2011; 30:1659–65. [PubMed: 21717507]
7. Bourgeois L, Gauriau C, Bernard JF. Projections from the nociceptive area of the central nucleus of the amygdala to the forebrain: a PHA-L study in the rat. *Eur J Neurosci*. 2001; 14:229–55. [PubMed: 11553276]
8. Calu DJ, Kawa AB, Marchant NJ, Navarre BM, Henderson MJ, Chen B, Yau HJ, Bossert JM, Schoenbaum G, Deisseroth K, Harvey BK, Hope BT, Shaham Y. Optogenetic inhibition of dorsal medial prefrontal cortex attenuates stress-induced reinstatement of palatable food seeking in female rats. *J Neurosci*. 2013; 33:214–26. [PubMed: 23283335]
9. Carrasquillo Y, Gereau RW. Activation of the extracellular signal-regulated kinase in the amygdala modulates pain perception. *J Neurosci*. 2007; 27:1543–51. [PubMed: 17301163]
10. Chai TC, Steers WD, Broder SR, Rauchenwald M, Tuttle JB. Characterization of laterality of innervation of the rat bladder. *Scand J Urol Nephrol Suppl*. 1996; 179:87–92. [PubMed: 8908671]
11. Chaplan SR, Bach FW, Pogrel JW, Chung JM, Yaksh TL. Quantitative assessment of tactile allodynia in the rat paw. *J Neurosci Methods*. 1994; 53:55–63. [PubMed: 7990513]
12. Coleman-Meschers K, Salinas JA, McGaugh JL. Unilateral amygdala inactivation after training attenuates memory for reduced reward. *Behav Brain Res*. 1996; 77:175–80. [PubMed: 8762168]
13. Crock LW, Kolber BJ, Morgan CD, Sadler KE, Vogt SK, Bruchas MR, Gereau RW. Central amygdala metabotropic glutamate receptor 5 in the modulation of visceral pain. *J Neurosci*. 2012; 32:14217–26. [PubMed: 23055491]
14. DeBerry JJ, Robbins MT, Ness TJ. The amygdala central nucleus is required for acute stress-induced bladder hyperalgesia in a rat visceral pain model. *Brain Res*. 2015; 1606:77–85. [PubMed: 25698616]
15. DeBerry JJ, Schwartz ES, Davis BM. TRPA1 mediates bladder hyperalgesia in a mouse model of cystitis. *PAIN*. 2014; 155:1280–7. [PubMed: 24704367]
16. Deutsch G, Deshpande H, Frolich MA, Lai HH, Ness TJ. Bladder distension increases blood flow in pain related brain structures in subjects with interstitial cystitis. *J Urol*. 2016; 196:902–10. [PubMed: 27018508]
17. Dixon WJ. The up-and-down method for small samples. *J Am Stat Assoc*. 1965; 60:967–78.
18. Dufour S, De Koninck Y. Optrodes for combined optogenetics and electrophysiology in live animals. *Neurophotonics*. 2015; 2:031205. [PubMed: 26158014]
19. Fields HL, Anderson SD, Clanton CH, Basbaum AI. Nucleus raphe magnus: a common mediator of opiate- and stimulus-produced analgesia. *Trans Am Neurol Assoc*. 1976; 101:208–10. [PubMed: 195380]
20. Ghirlanda S, Vallortigara G. The evolution of brain lateralization: a game-theoretical analysis of population structure. *Proc Biol Sci*. 2004; 271:853–7. [PubMed: 15255105]

21. Goncalves L, Dickenson AH. Asymmetric time-dependent activation of right central amygdala neurones in rats with peripheral neuropathy and pregabalin modulation. *Eur J Neurosci.* 2012; 36:3204–13. [PubMed: 22861166]
22. Han JS, Neugebauer V. Synaptic plasticity in the amygdala in a visceral pain model in rats. *Neurosci Lett.* 2004; 361:254–7. [PubMed: 15135941]
23. Ji G, Neugebauer V. Hemispheric lateralization of pain processing by amygdala neurons. *J Neurophysiol.* 2009; 102:2253–64. [PubMed: 19625541]
24. Kleinhans NM, Yang CC, Strachan ED, Buchwald DS, Maravilla KR. Alterations in connectivity on functional magnetic resonance imaging with provocation of lower urinary tract symptoms: a MAPP Research Network Feasibility Study of Urological Chronic Pelvic Pain Syndromes. *J Urol.* 2016; 195:639–45. [PubMed: 26497778]
25. Kwon JK, Chang IH. Pain, catastrophizing, and depression in chronic prostatitis/chronic pelvic pain syndrome. *Int Neurourol J.* 2013; 17:48–58. [PubMed: 23869268]
26. Lu A, Steiner MA, Whittle N, Vogl AM, Walser SM, Ableitner M, Refojo D, Ekker M, Rubenstein JL, Stalla GK, Singewald N, Holsboer F, Wotjak CT, Wurst W, Deussing JM. Conditional mouse mutants highlight mechanisms of corticotropin-releasing hormone effects on stress-coping behavior. *Mol Psychiatry.* 2008; 13:1028–42. [PubMed: 18475271]
27. Martucci KT, Shirer WR, Bagarinao E, Johnson KA, Farmer MA, Labus JS, Apkarian AV, Deutsch G, Harris RE, Mayer EA, Clauw DJ, Greicius MD, Mackey SC. The posterior medial cortex in urologic chronic pelvic pain syndrome: detachment from default mode network—a resting-state study from the MAPP Research Network. *PAIN.* 2015; 156:1755–64. [PubMed: 26010458]
28. Missig G, Roman CW, Vizzard MA, Braas KM, Hammack SE, May V. Parabrachial nucleus (PBN) pituitary adenylate cyclase activating polypeptide (PACAP) signaling in the amygdala: implication for the sensory and behavioral effects of pain. *Neuropharmacology.* 2014; 86:38–48. [PubMed: 24998751]
29. Naliboff BD, Berman S, Chang L, Derbyshire SW, Suyenobu B, Vogt BA, Mandelkern M, Mayer EA. Sex-related differences in IBS patients: central processing of visceral stimuli. *Gastroenterology.* 2003; 124:1738–47. [PubMed: 12806606]
30. Ness TJ. Evidence for ascending visceral nociceptive information in the dorsal midline and lateral spinal cord. *PAIN.* 2000; 87:83–8. [PubMed: 10863048]
31. Ness TJ, Elhefni H. Reliable visceromotor responses are evoked by noxious bladder distention in mice. *J Urol.* 2004; 171:1704–8. [PubMed: 15017270]
32. Ness TJ, Richter HE, Varner RE, Fillingim RB. A psychophysical study of discomfort produced by repeated filling of the urinary bladder. *PAIN.* 1998; 76:61–9. [PubMed: 9696459]
33. Neugebauer V, Li W, Bird GC, Han JS. The amygdala and persistent pain. *Neuroscientist.* 2004; 10:221–34. [PubMed: 15155061]
34. Nickel JC, Tripp DA, Pontari M, Moldwin R, Mayer R, Carr LK, Doggweiler R, Yang CC, Mishra N, Nordling J. Psychosocial phenotyping in women with interstitial cystitis/painful bladder syndrome: a case control study. *J Urol.* 2010; 183:167–72. [PubMed: 19913812]
35. Nishii H, Nomura M, Aono H, Fujimoto N, Matsumoto T. Up-regulation of galanin and corticotropin-releasing hormone mRNAs in the key hypothalamic and amygdaloid nuclei in a mouse model of visceral pain. *Regul Pept.* 2007; 141:105–12. [PubMed: 17335920]
36. Pascual JI, Insausti R, Gonzalo LM. Urinary bladder innervation in male rat: termination of primary afferents in the spinal cord as determined by transganglionic transport of WGA-HRP. *J Urol.* 1993; 150(2 pt 1):500–4. [PubMed: 7686986]
37. Paur I, Balstad TR, Kolberg M, Pedersen MK, Austenaa LM, Jacobs DR Jr, Blomhoff R. Extract of oregano, coffee, thyme, clove, and walnuts inhibits NF-kappaB in monocytes and in transgenic reporter mice. *Cancer Prev Res.* 2010; 3:653–63.
38. Paxinos, G., Franklin, K. Paxinos and Franklin's the mouse brain in stereotaxic coordinates. Cambridge, MA: Academic Press; 2012.
39. Rizvi TA, Ennis M, Behbehani MM, Shipley MT. Connections between the central nucleus of the amygdala and the midbrain periaqueductal gray: topography and reciprocity. *J Comp Neurol.* 1991; 303:121–31. [PubMed: 1706363]

40. Rodrigues SM, Bauer EP, Farb CR, Schafe GE, LeDoux JE. The group I metabotropic glutamate receptor mGluR5 is required for fear memory formation and long-term potentiation in the lateral amygdala. *J Neurosci*. 2002; 22:5219–29. [PubMed: 12077217]
41. Sadler KE, Stratton JM, DeBerry JJ, Kolber BJ. Optimization of a pain model: effects of body temperature and anesthesia on bladder nociception in mice. *PLoS One*. 2013; 8:e79617. [PubMed: 24223980]
42. Sadler KE, Stratton JM, Kolber BJ. Urinary bladder distention evoked visceromotor responses as a model for bladder pain in mice. *J Vis Exp*. 2014; 86:e51413.
43. Smith Y, Pare D. Intra-amygdaloid projections of the lateral nucleus in the cat: PHA-L anterograde labeling combined with postembedding GABA and glutamate immunocytochemistry. *J Comp Neurol*. 1994; 342:232–48. [PubMed: 7911130]
44. Sorge RE, Martin LJ, Isbester KA, Sotocinal SG, Rosen S, Tuttle AH, Wieskopf JS, Acland EL, Dokova A, Kadoura B, Leger P, Mapplebeck JC, McPhail M, Delaney A, Wigerblad G, Schumann AP, Quinn T, Frasnelli J, Svensson CI, Sternberg WF, Mogil JS. Olfactory exposure to males, including men, causes stress and related analgesia in rodents. *Nat Methods*. 2014; 11:629–32. [PubMed: 24776635]
45. Stillwell TJ, Benson RC Jr. Cyclophosphamide-induced hemorrhagic cystitis. A review of 100 patients. *Cancer*. 1988; 61:451–7. [PubMed: 3338015]
46. Tran L, Greenwood-Van Meerveld B. Lateralized amygdala activation: importance in the regulation of anxiety and pain behavior. *Physiol Behav*. 2012; 105:371–5. [PubMed: 21925523]
47. Tronche F, Kellendonk C, Kretz O, Gass P, Anlag K, Orban PC, Bock R, Klein R, Schutz G. Disruption of the glucocorticoid receptor gene in the nervous system results in reduced anxiety. *Nat Genet*. 1999; 23:99–103. [PubMed: 10471508]
48. Tye KM, Prakash R, Kim SY, Fenno LE, Grosenick L, Zarabi H, Thompson KR, Gradinaru V, Ramakrishnan C, Deisseroth K. Amygdala circuitry mediating reversible and bidirectional control of anxiety. *Nature*. 2011; 471:358–62. [PubMed: 21389985]
49. Vaudry D, Falluel-Morel A, Bourgault S, Basille M, Burel D, Wurtz O, Fournier A, Chow BK, Hashimoto H, Galas L, Vaudry H. Pituitary adenylate cyclase-activating polypeptide and its receptors: 20 years after the discovery. *Pharmacol Rev*. 2009; 61:283–357. [PubMed: 19805477]
50. Willis WD, Westlund KN. Neuroanatomy of the pain system and of the pathways that modulate pain. *J Clin Neurophysiol*. 1997; 14:2–31. [PubMed: 9013357]
51. Yizhar O, Fenno Lief E, Davidson Thomas J, Mogri M, Deisseroth K. Optogenetics in neural systems. *Neuron*. 2011; 71:9–34. [PubMed: 21745635]
52. Zhang F, Gradinaru V, Adamantidis AR, Durand R, Airan RD, de Lecea L, Deisseroth K. Optogenetic interrogation of neural circuits: technology for probing mammalian brain structures. *Nat Protoc*. 2010; 5:439–56. [PubMed: 20203662]

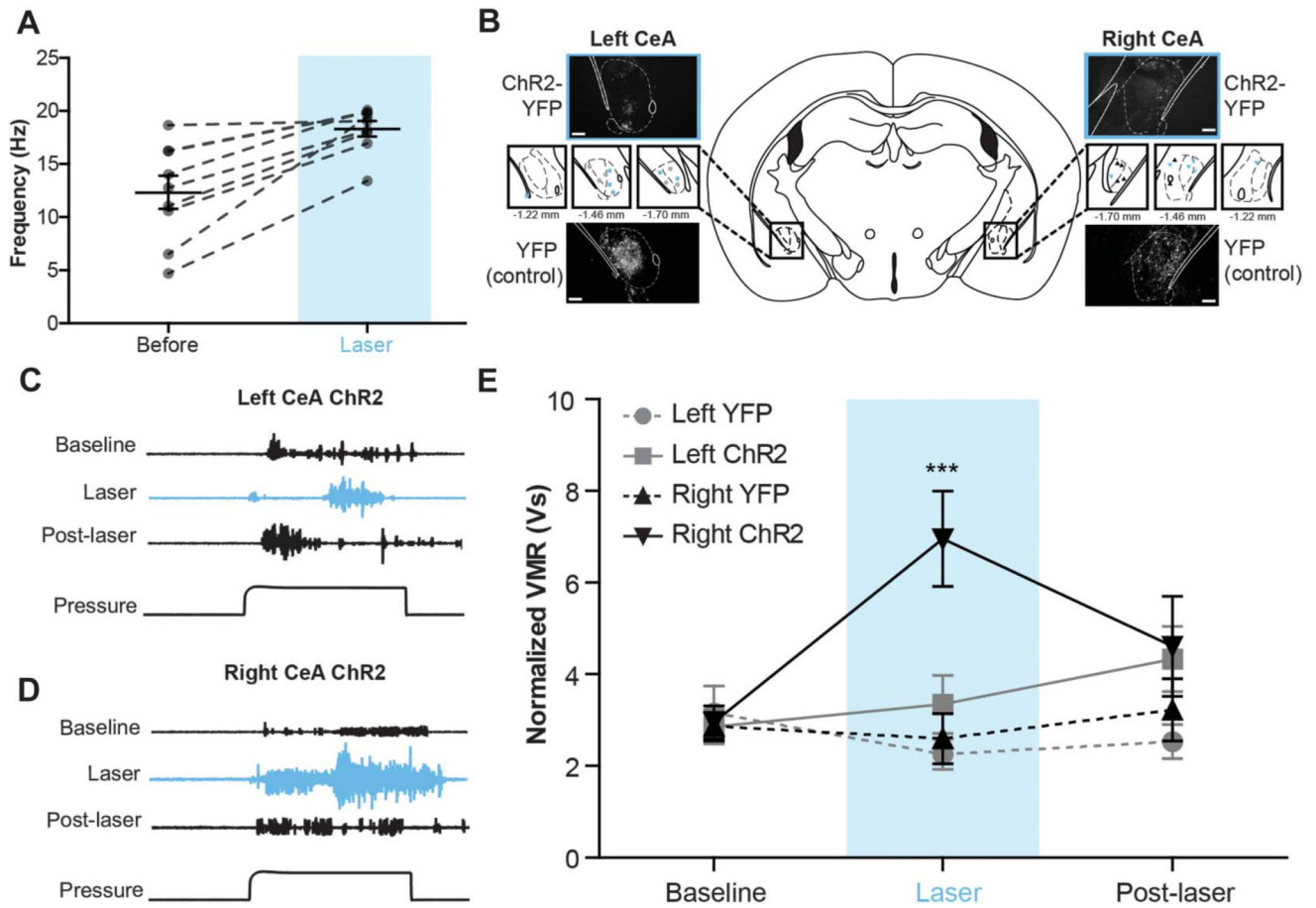


Figure 1. Optogenetic activation of the right central amygdala (CeA) increases pain-like responses to noxious bladder distension

(A) Pulsing 473-nm light at 20 Hz significantly increased firing rates of neurons in channelrhodopsin-2 (ChR2)-expressing regions of the CeA (paired t test, $P = 0.0009$; $n = 9$).

(B) Three weeks after targeted viral injections, nestin-Cre mice expressed either yellow fluorescent protein (YFP)-tagged ChR2 or YFP alone in the left or right CeA (scale bar, 0.1 mm). Targeting for all experimental and control animals is shown in insets (blue ■, left ChR2-YFP; gray ●, left YFP; blue ▼, right ChR2-YFP; gray ▲, right YFP).

(C) Representative traces show electromyographic responses to noxious bladder distension (60 mm Hg) prior to, during, and after laser-induced activation of ChR2-expressing neurons in the left CeA. Optogenetic activation failed to produce significant qualitative changes in abdominal muscle output.

(D) Optogenetic activation of the right CeA induced marked increases in abdominal muscle contraction during bladder distension.

(E) Optogenetic activation of the right CeA significantly increased visceromotor responses (VMRs) (2-way repeated measures analysis of variance effect of group, $P = 0.0296$; effect of time, $P = 0.0330$; group \times time interaction, $P = 0.0001$; Bonferroni posttest right ChR2 vs right YFP at laser, $***P < 0.001$; right ChR2 laser vs baseline, $***P < 0.001$; right ChR2 vs left ChR2 at laser, $***P < 0.001$; $n = 6$ in each group). Optogenetic activation of the left CeA had no significant effect on VMRs during bladder distension, and likewise, laser stimulation in control groups had no effect on VMRs. Fifteen minutes after the end of laser stimulation,

VMRs for all experimental and control groups were similar to each other and not significantly different from baseline responses.

Author Manuscript

Author Manuscript

Author Manuscript

Author Manuscript

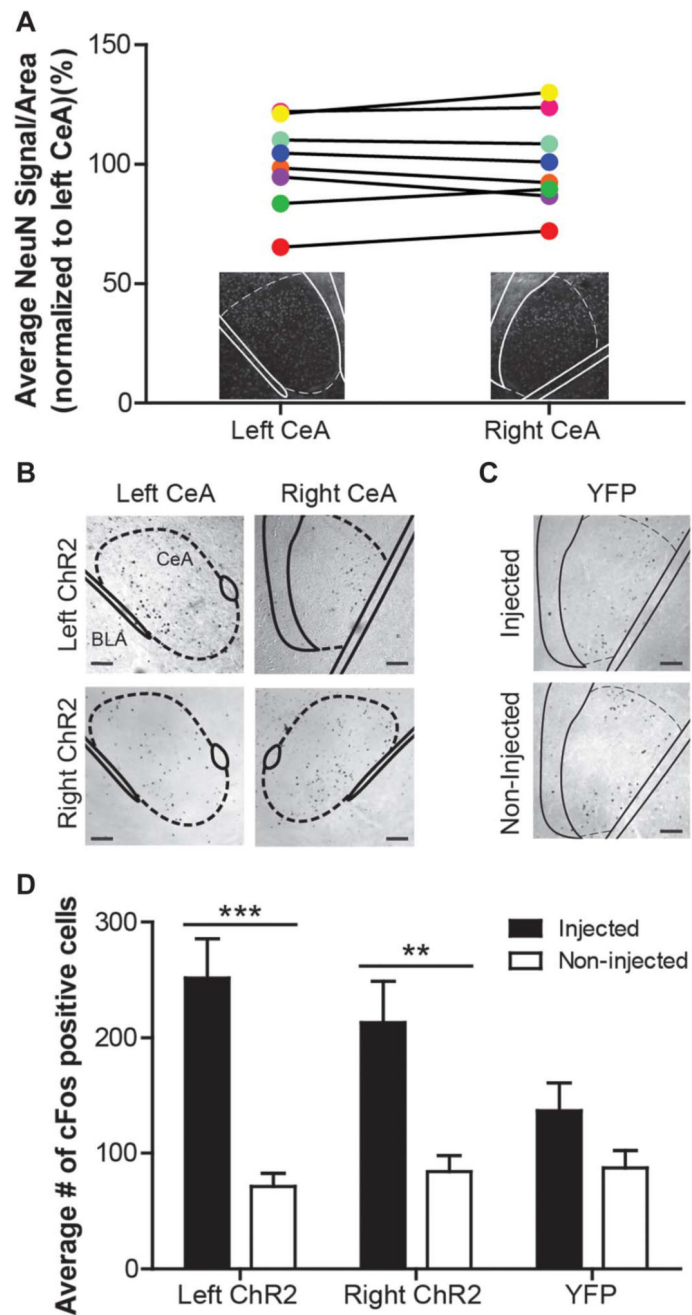


Figure 2. Left and right central amygdalae (CeA) do not differ in neuron number or activation levels during channelrhodopsin-2 (ChR2)-mediated depolarization
 (A) NeuN staining was used to determine the number of neurons in the left and right CeA of naive C57Bl/6 animals. The NeuN signal does not differ between nuclei (paired *t* test, $P=0.8238$; $n=8$); matching colored symbols represent the average left and right signal from one animal. Insets show representative images of each nucleus. (B) The left and right CeA of animals expressing ChR2-yellow fluorescent protein (YFP) were stained for cFos after optogenetic stimulation and urinary bladder distension. cFos-positive cells are predominantly located in the CeA (scale bar, 0.1 mm). (C) cFos was also examined in both the injected and noninjected sides of brains from animals expressing YFP alone (scale bar,

0.1 mm). (D) Both left ChR2 (n = 11) and right ChR2 (n = 7)-expressing nuclei exhibited increases in cFos expression when compared with their nonstimulated counternuclei (2-way repeated measures analysis of variance effect of injection, $P < 0.0001$; group \times injection interaction, $P = 0.0144$; Bonferroni posttest for left ChR2 injected vs noninjected, $***P < 0.001$; right ChR2 injected vs noninjected, $**P < 0.01$). Additionally, the activation levels between these left and right stimulated nuclei do not differ. In YFP-expressing brains (n = 6), there is no significant difference in cFos expression between injected and noninjected nuclei.

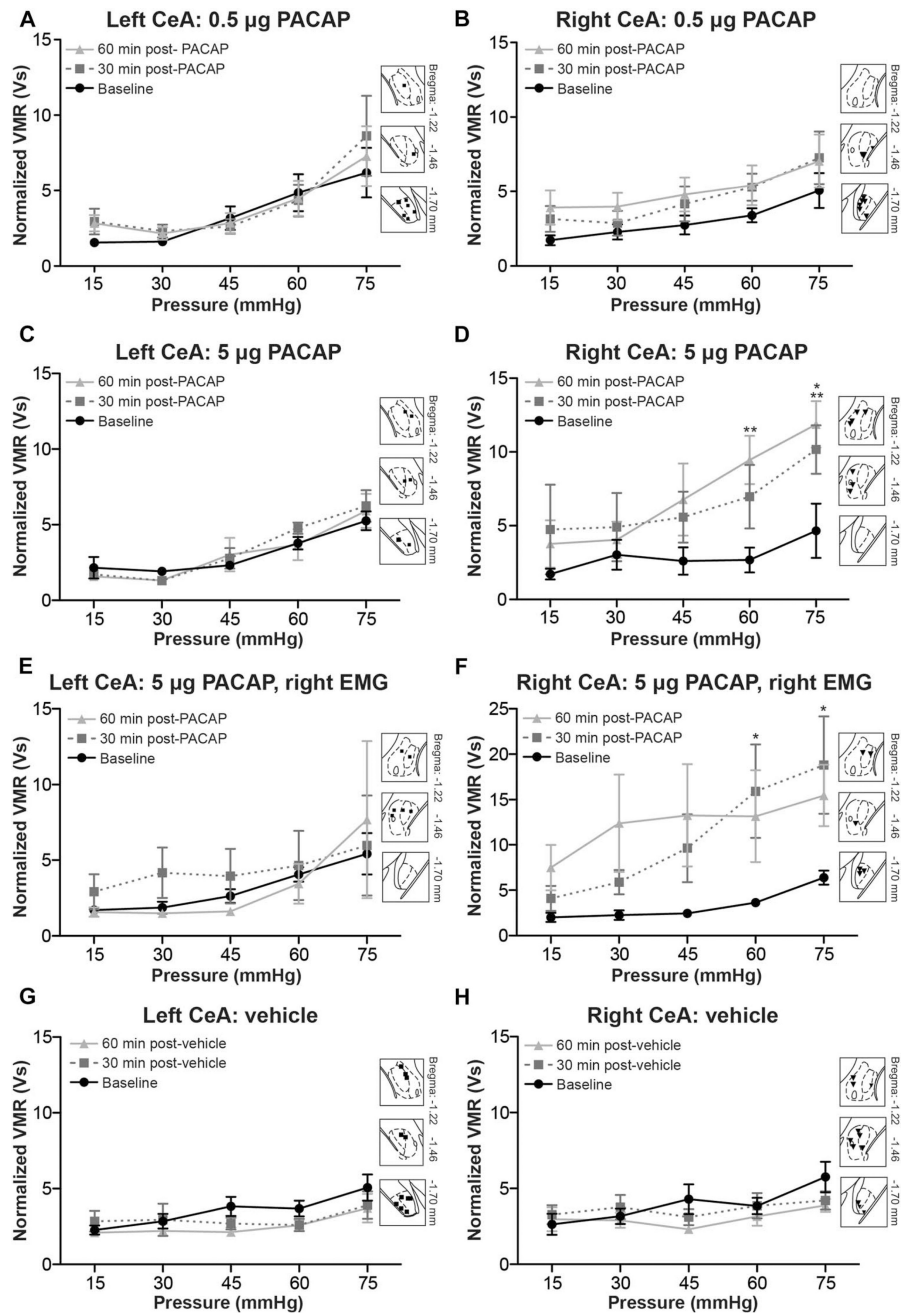


Figure 3. Pituitary adenylate cyclase-activating polypeptide (PACAP) administration in the right central amygdala (CeA), and not the left, increases responses to bladder distension. Two doses of PACAP were administered into the left or right CeA after one round of graded urinary bladder distension (UBD)

(A) Infusion of 0.5 μ g PACAP into the left CeA failed to change visceromotor responses (VMRs) 30 or 60 minutes after application (2-way repeated measures [RM] analysis of variance [ANOVA] effect of pressure, $P = 0.0041$; $n = 9$) Insets show targeting of the left CeA. (B) Infusion of 0.5 μ g PACAP in the right CeA significantly increased VMRs (2-way RM ANOVA effect of treatment, $P = 0.0021$; effect of pressure, $P = 0.0220$; $n = 9$). Insets show targeting of the right CeA. (C) Infusion of 5 μ g PACAP dose in the left CeA failed to

significantly change VMRs obtained from the left abdominal muscle 30 or 60 minutes after application (2-way RM ANOVA effect of pressure, $P < 0.0001$; $n = 6$). (D) Infusion of 5 μg PACAP into the right CeA resulted in statistically significant increases in UBD VMRs recorded from the left abdominal muscle, specifically at the most noxious intravesical pressures (2-way RM ANOVA effect of treatment, $P < 0.0001$; effect of pressure, $P = 0.0767$; Bonferroni posttest for baseline vs 30 minutes, $*P < 0.05$; for baseline vs 60 minutes, $**P < 0.01$; $n = 6$). (E) VMRs from the right abdominal muscle did not change after administration of 5 μg PACAP in the left CeA. (F) Infusion of 5 μg PACAP in the right CeA causes a robust increase in UBD-evoked VMRs recorded from the right abdominal muscle (2-way RM ANOVA effect of treatment, $P < 0.0001$; $n = 6$). Significant increases in UBD-evoked VMRs were noted 30 minutes after PACAP administration (Bonferroni posttest for baseline vs 30 minutes, $*P < 0.05$ at 60 and 75 mm Hg). (G, H) To control for microinjection manipulation and time elapsed during procedure, vehicle (0.05% bovine serum albumin in saline) was applied into the left or right CeA in a third group of animals. No change in VMR occurred 30 or 60 minutes after vehicle application in either (G) the left CeA (2-way RM ANOVA effect of pressure, $P = 0.0001$; $n = 11$) or (H) the right CeA (2-way RM ANOVA effect of pressure, $P = 0.0034$; $n = 10$).

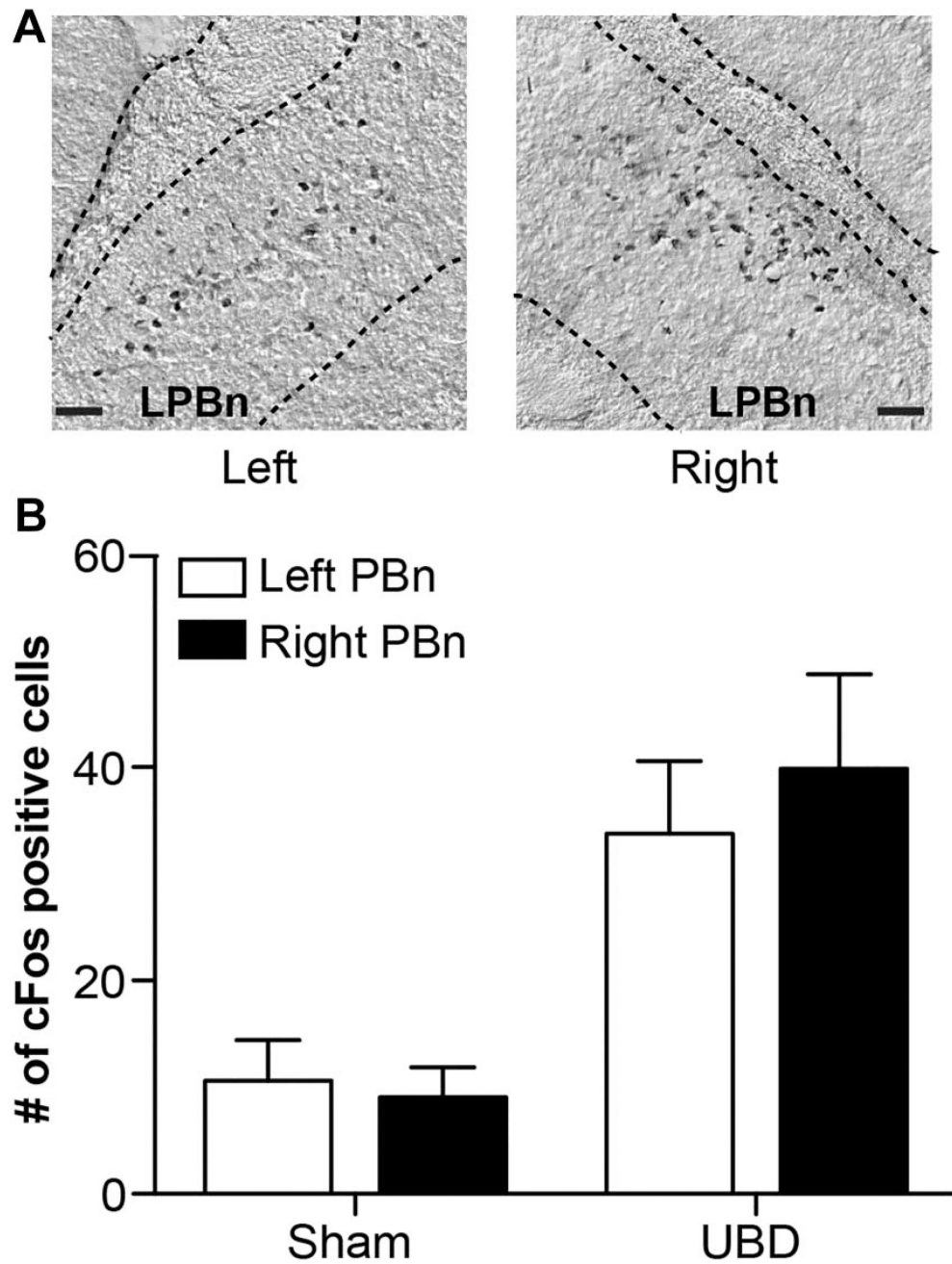


Figure 4. Graded bladder distension equally activates left and right para-brachial nucleus (PBn) (A) cFos-positive neurons were localized to the left and right lateral PBn after one round of graded bladder distension. (B) Urinary bladder distension (UBD) significantly and equivalently increased the number of cFos-positive cells in the left and right PBn compared with sham animals (2-way repeated measures analysis of variance effect of UBD, $P=0.0018$; $n=6$; scale bar, 0.05 mm).

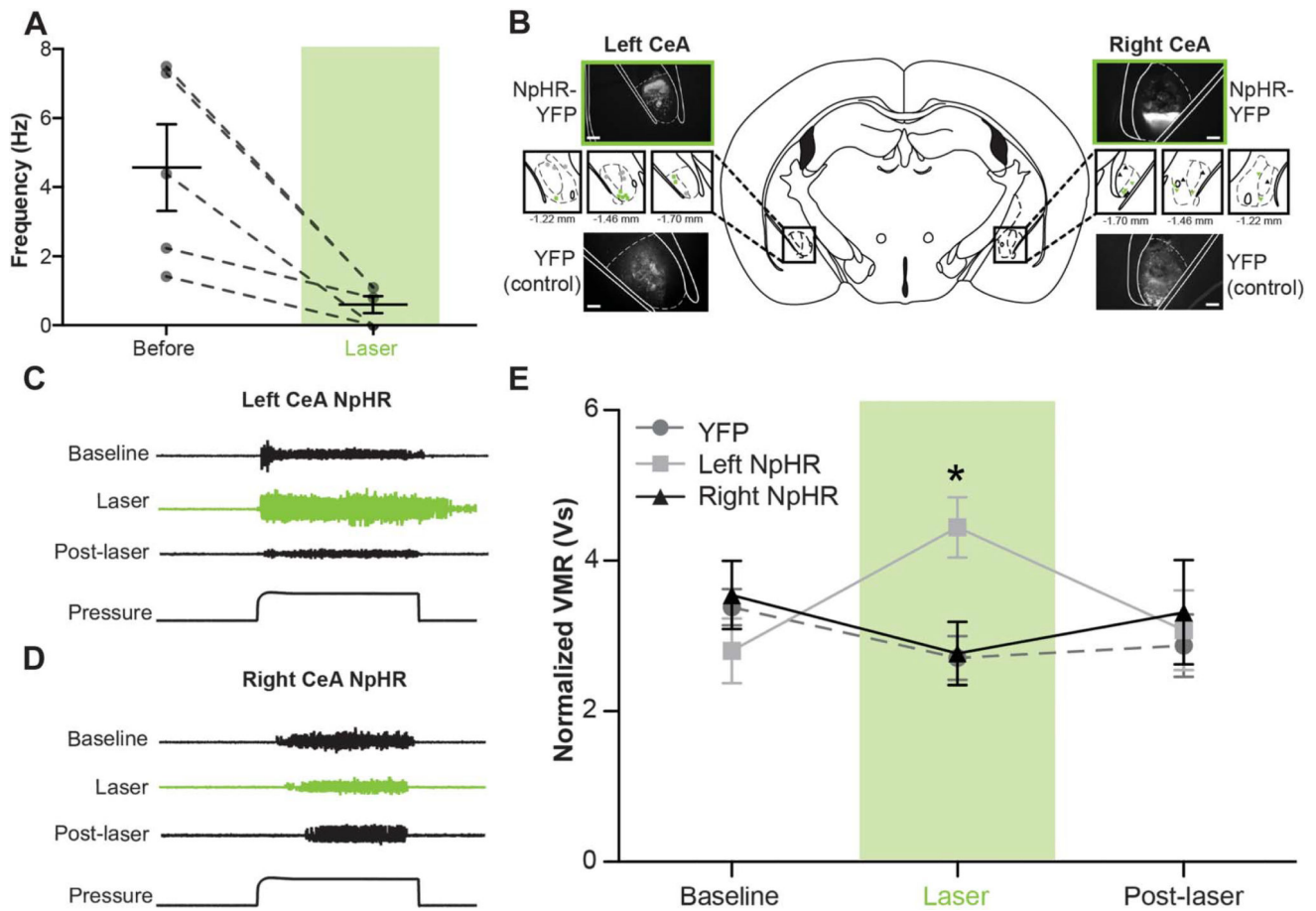


Figure 5. Optogenetic inhibition of the left central amygdala (CeA) increases pain-like responses to noxious bladder distension

(A) Constant application of 532-nm light in NpHR-expressing regions of the CeA significantly decreased neuronal firing rates (paired t test, $P = 0.0224$; $n = 5$). (B) Three weeks after targeted viral injections, nestin-Cre mice expressed either yellow fluorescent protein (YFP)-tagged NpHR or YFP alone in the left or right CeA (scale bar, 0.1 mm). Targeting for all experimental and control animals is shown in insets (green ■, left NpHR-YFP; gray ●, left YFP; green ▼, right NpHR-YFP; gray ▲, right YFP). (C) Representative electromyographic (EMG) traces show qualitative changes during left CeA optogenetic inhibition. (D) Representative EMG traces fail to show qualitative changes during right CeA optogenetic inhibition. (E) Quantified visceromotor responses (VMRs) show that optogenetic inhibition of the left CeA significantly increased responses to urinary bladder distension when compared with VMRs obtained during right CeA inhibition or optical stimulation in YFP-expressing CeA (2-way repeated measures analysis of variance group \times time interaction, $P = 0.0126$; Bonferroni posttest left NpHR vs right NpHR at laser, $*P < 0.05$, left NpHR vs YFP at laser, $*P < 0.05$, left NpHR laser vs baseline, $*P < 0.05$; $n = 9-19$). Fifteen minutes after the end of laser stimulation, VMRs were once again equivalent between groups and not different from baseline responses.

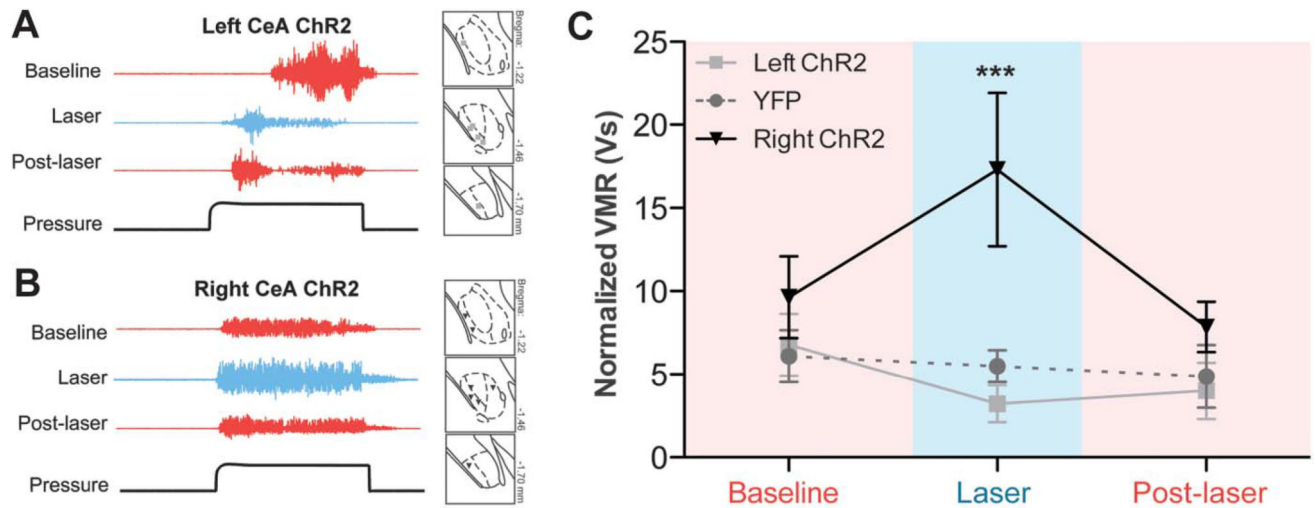


Figure 6. Optogenetic activation of the right central amygdala (CeA) in bladder-sensitized mice further increases bladder nociception. After cyclophosphamide treatment, animals expressing channelrhodopsin-2 (ChR2) in the left or right CeA were placed through 3 rounds of noxious (60 mm Hg) bladder distension

(A) Representative electromyographic (EMG) traces during optogenetic activation of the left CeA. Insets illustrate viral targeting in the CeA (gray ■, left ChR2). (B) Representative EMG traces during right CeA optogenetic activation display increases in visceromotor responses (VMRs). Insets illustrate viral targeting in the CeA (black ▼, right ChR2). (C) In bladder-sensitized animals, optogenetic activation of the right CeA significantly increased urinary bladder distension–evoked VMRs (2-way repeated measures analysis of variance overall effect of group, $P = 0.0218$; group \times time interaction, $P = 0.0264$; Bonferroni posttest for right ChR2 vs yellow fluorescent protein (YFP) at laser, $**P < 0.01$; right ChR2 vs left ChR2 at laser, $***P < 0.001$; right ChR2 baseline vs laser, $*P < 0.05$; $n = 5-7$). Laser stimulation in YFP-expressing control mice had no effect on VMRs.

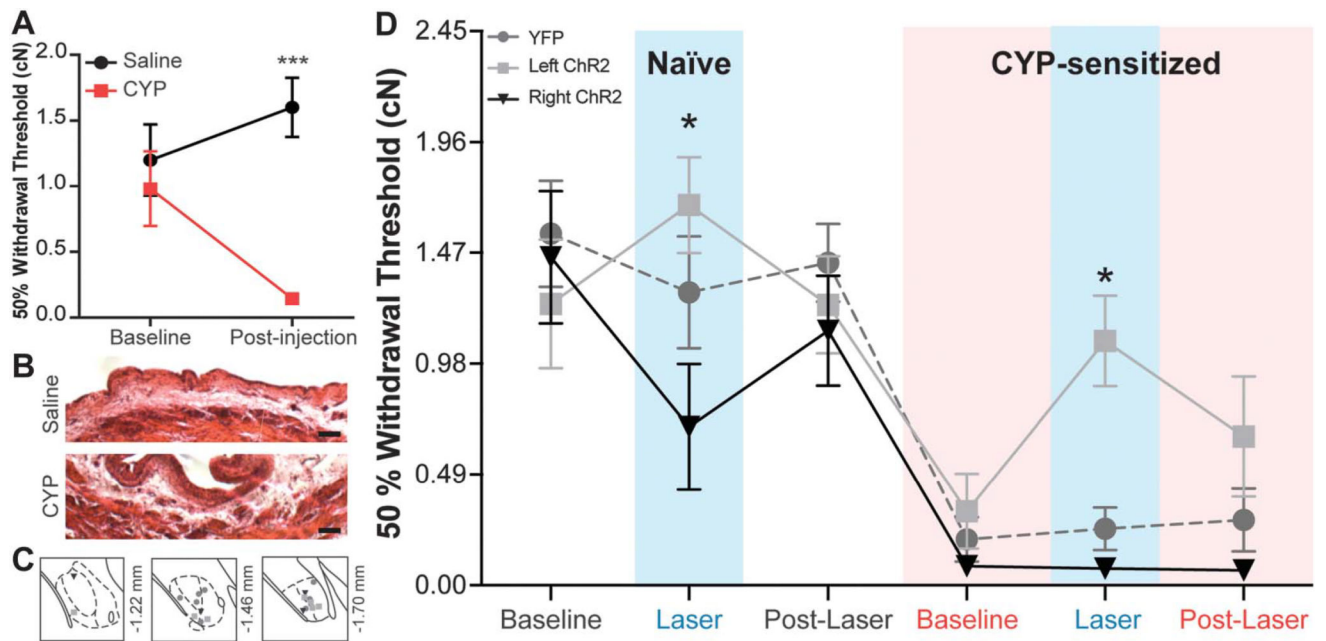


Figure 7. Activation of the right central amygdala (CeA) increases naive abdominal sensitivity while activation of the left CeA reverses referred bladder pain. Five days of cyclophosphamide (CYP) treatment induces referred bladder pain as measured by von Frey filaments (A) CYP-treated animals display a statistically significant decrease in abdominal withdrawal threshold when compared with saline-treated animals (2-way repeated measures [RM] analysis of variance [ANOVA] overall effect of CYP, $P = 0.0042$; effect of interaction, $P = 0.0030$; Bonferroni posttest CYP vs saline at postinjection, $***P < 0.001$; $n = 12$). (B) CYP-treated animals display noticeable edema in the submucosal layers of the bladder and thickening of the urothelium (scale bar, $50 \mu\text{m}$). (C) channelrhodopsin-2 (ChR2) and yellow fluorescent protein (YFP) vectors were successfully targeted to the left or right CeA (gray \bullet , YFP; light gray \blacksquare , left ChR2; black \blacktriangledown , right ChR2). (D) In naive animals, optogenetic activation of the right CeA causes a significant decrease in withdrawal threshold compared with the effects of left CeA activation ($n = 6-9$; 2-way ANOVA effect of group, $P = 0.0017$; Bonferroni posttest right ChR2 vs left ChR2 at naive laser, $*P < 0.05$), suggesting divergent effects of the 2 nuclei. Withdrawal thresholds of each group do not differ prior to and after laser-induced activation of either nucleus. After 5 days of CYP treatment, all groups exhibit referred bladder pain as indicated by significantly reduced mechanical withdrawal thresholds (2-way RM ANOVA effect of time, $P < 0.0001$; Bonferroni posttest naive baseline vs CYP baseline for YFP, $P < 0.0001$; for left ChR2, $P < 0.05$; for right ChR2, $P < 0.01$). Optogenetic activation of the right CeA has no assessable effect on withdrawal thresholds in sensitized animals. Optogenetic activation of the left CeA during CYP sensitization reverses referred bladder pain (Bonferroni posttest left ChR2 vs right ChR2 at CYP laser, $*P < 0.05$).